CONF-970246--1

Circumference imaging for optical based identification of cylindrical and conical objects

Martin A. Hunt, David N. Sitter, Regina K. Ferrell, and J. Eric Breeding

Oak Ridge National Laboratory[1], MS 6011, Oak Ridge, TN 37831

RECEIVED
FEB 06 1997
OSTI

ABSTRACT

Inspection and identification of cylindrical or conical shaped objects presents a unique challenge for a machine vision system. Due to the circular nature of the objects it is difficult to image the whole object using traditional area cameras and image capture methods. This work describes a unique technique to acquire a two dimensional image of the entire surface circumference of a cylindrical/conical shaped object. The specific application of this method is the identification of large caliber (155 mm) ammunition rounds in the field as they are transported between or within vehicles. The proposed method utilizes a line scan camera in combination with high speed image acquisition and processing hardware to acquire images from multiple cameras and generate a single, geometrically accurate, surface image. The primary steps involved are the capture of multiple images as the ammunition moves by on the conveyor followed by warping to correct for the distortion induced by the curved projectile surface. The individual images are then tiled together to form one two-dimensional image of the complete circumference. Once this image has been formed an automatic identification algorithm begins the feature extraction and classification process.

Keywords: Geometric warping, object identification, circumference imaging, real-time processing, optical distortion

1. INTRODUCTION

In many electronic imaging applications the object to be captured for subsequent analysis is not a simple geometric shape with flat surfaces perpendicular to the camera's axis. Some applications can either tolerate optical geometric distortions due to irregularly shaped objects or provide calibration procedures to compensate for the fixed distortions. However, one particular application which requires a dynamic correction of the optical distortion is the generation of a circumference image of a cylindrical object with varying radius and length. In this application several factors determine the optical distortions including curvature of the object, which affects the object distance and variable spatial resolution, and the object radius, which also affects the object distance. This paper will focus on the dynamic correction of the optical distortions experienced in acquiring cylindrical/conical objects and the process of creating a mosaic or composite image of the entire circumference of the object's surface.

The specific application of this method is the identification of large caliber (155 mm) ammunition rounds in the field as they are transported between or within vehicles. The entire circumference of the round must be imaged because the angular orientation can not be controlled. Text and other markings could be located anywhere on the round including the conical section of the tip. A line scan approach is used due to the axial motion of the round during transport (typically on a V conveyor belt).

The process of geometric or spatial transformations has been used extensively in the fields of satellite imaging and mapping,[1-3] medical imaging,[4-6] and image enhancement.[7-8] Several texts[9-10] cover the topic of image warping or geometric transformations. In general this process is broken into two phases: a spatial transformation and an interpolation of the new

---

[1] Work performed for U.S. Army Program Manager - Crusader by OAK RIDGE NATIONAL LABORATORY, Oak Ridge, Tennessee, 37831-6285, managed by LOCKHEED MARTIN ENERGY RESEARCH CORP. for the U.S. DEPARTMENT OF ENERGY under contract DE-AC05-96OR22464.

Correspondence: M. A. Hunt. Additional author information: M.A.H: Email: huntma@ornl.gov; WWW: http://www-ismv.ic.ornl.gov; Telephone: 523-574-5743; Fax: 423-574-6663

DISTRIBUTION OF THIS DOCUMENT IS UNLIMITED

MASTER

DISCLAIMER

This report was prepared as an account of work sponsored by an agency of the United States Government. Neither the United States Government nor any agency thereof, nor any of their employees, make any warranty, express or implied, or assumes any legal liability or responsibility for the accuracy, completeness, or usefulness of any information, apparatus, product, or process disclosed, or represents that its use would not infringe privately owned rights. Reference herein to any specific commercial product, process, or service by trade name, trademark, manufacturer, or otherwise does not necessarily constitute or imply its endorsement, recommendation, or favoring by the United States Government or any agency thereof. The views and opinions of authors expressed herein do not necessarily state or reflect those of the United States Government or any agency thereof.

DISCLAIMER

Portions of this document may be illegible in electronic image products. Images are produced from the best available original document.

pixel values. The spatial transformation can be a polynomial mapping of a set of tie-points or targets from one image domain to the corresponding points in another image or map coordinate.[11-12] Another method uses the known physical properties of the image acquisition system or object to generate an analytical transform of the desired transformation.[13-14] In this application the optical properties of the imaging system can be exploited to define a spatial transformation based on measurable attributes within the image. The unique feature of this approach is that the dynamic measurements can be made invariant to the geometric distortions encountered.

The primary steps involved in the circumference imaging process are the capture of four individual images (each camera would image one quarter of the circumference) as the ammunition moves by a viewing gap between two conveyor segments. Next the resulting lines are warped to correct for the distortion induced by the curved projectile surface, then the four individual images are tiled together to form one two dimensional image of the complete circumference. Once this image has been formed the identification algorithm would begin the feature extraction and classification process. Also, the expected image location that contained text would be extracted and processed by a character recognition algorithm.

2. GEOMETRIC WARPING

The optical system images the curved surface of the ammunition shell onto a linear detector array. The imaged line on the shell is perpendicular to the axis of the shell. Because of the camera's perspective relative to the curved surface, detail on the shell surface becomes spatially compressed in the image near the left and right edges of the shell. Figure 1 illustrates the image of a shell captured from a single camera. Note how the text information appears compressed in the image near the edges of the shell. Because character recognition software is sensitive to the size and shape of text in images, the distorted image of the shell must first be "unwarped." Otherwise, errors in reading the text will occur. In this section, the equations for unwarping the image are given.

Figure 2 illustrates the geometry of the problem. The lens in the camera is modeled as a thin, distortion-free lens with focal length, f. The ammunition shell has a radius of R which changes along the length of the shell. The lens is focused on the plane, perpendicular to the optical axis, which intersects the vertex of a nominal shell radius denoted $\overline{R}$. Object points lying in front of or behind this plane become progressively more out-of-focus. At the fixed nominal radius $\overline{R}$ the lateral magnification of the lens is given by $\overline{M}$. The arc height of the object along the shell surface is given by $\tilde{h}_o$, and the corresponding height of the image point on the detector array is given by h_i. One can show that the arc height on the shell is related to the image height on the sensor by the following equation

$$h_i = \frac{\overline{d}_i \, Sin\left(\tilde{h}_o / R\right)}{L - R\,Cos\left(\tilde{h}_o / R\right)}, \tag{1}$$

where

$$\overline{d}_i = \left(\overline{M} + 1\right) f, \tag{2}$$

and

$$L = \left(\overline{M} + 1\right) f / \overline{M} + \overline{R}. \tag{3}$$

In order to use Eq. (1) effectively, the focal length of the lens f, the nominal magnification $\overline{M}$, and the nominal radius of focus $\overline{R}$ should be accurately known. In addition, the radius R at every imaged line must be determined. A method to determine the physical radius from a line image is given in Section 3.

Original Warped

Figure 1 Two images of original scan and warped segment prior to tiling. The text appears distorted near the edges of the shell (Note the numeral 4 in the lower right portion of the image). The warped image has been cropped to one quarter of the total circumference.

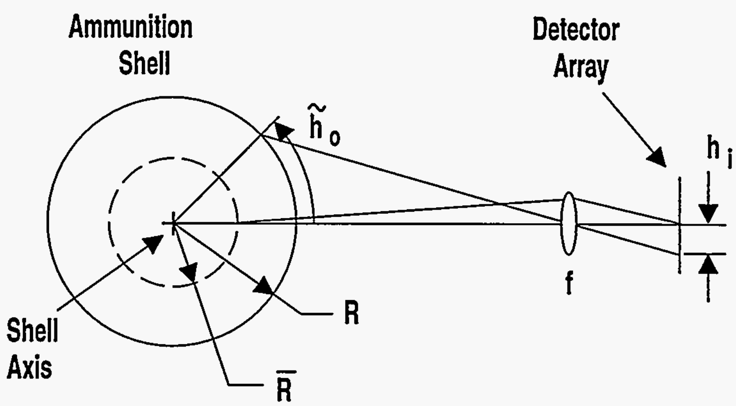

Figure 2. Geometry of the optical imaging system. (Only a single camera is shown.)

The image is undistorted by substituting the desired arc height $\tilde{h}_o$ along the curved surface into Eq. (1) and determining the physical height h_i on the image sensor. This a target to source mapping used to generate the value of the pixel in the target domain by locating, using Eq. (1), the location of the pixel in the source domain. During the unwarping procedure, the spatial resolution on the shell in the unwarping routine is held constant. The size of the imaged detector on the nominal plane of focus is simply given by

$$\Delta_o = \Delta_i / \overline{M}, \qquad (4)$$

where Δ_i is the distance between detector elements on the sensor. An undistorted image can be built up by repeatedly applying Eq.(1) with the arc-length determined by

$$\tilde{h}_o = n\,\Delta_o, \qquad \{n = 0, \pm 1, \pm 2, \ldots, \pm N_{\max}). \qquad (5)$$

Figure 1 shows the results of this algorithm for a given actual scan shown in the left image and the undistorted image on the right.

3. IMAGE TILING

Multiple cameras surrounding the ammunition shell are used to build up an image of the entire circumference of the shell. Each camera is used to map a 360°/ N_c arc of the surface, where N_c is the number of cameras used. Since the spatial resolution on the shell surface is held constant, the number of pixels covering the shell circumference decreases as the shell radius decreases. The number of pixels in the corrected image from the center of the field of view to the cross-over point between adjacent cameras is given by

$$N_{\max}(R) = \left[\frac{R\pi}{\Delta_o N_c} \right]_{\text{integer}}, \qquad (6)$$

where the square brackets function, $[\cdot]_{\text{integer}}$, indicates the selection of the nearest integer.

As the shell radius changes, the point in the camera's field of view which represents the cross-over location or the "seam" between the images of adjacent camera system changes. Figure 3 illustrates this point. The cross-over location for different radii is imaged to a different location on the sensor array. Thus, in order to tile the N_c images together the cross-over point must be determined for every line image. This requires the physical radius of the shell to be determined.

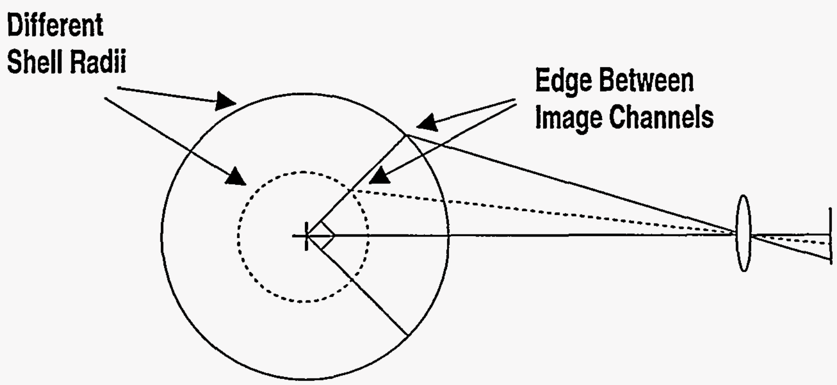

Figure 3. In a four-camera system (only one is shown) each camera is used to map 90° of the surface. As the radius decreases, the location of the cross-over point in the image changes.

The physical radius of the shell for a given line image can be determined in the following way. Figure 4 illustrates the geometry of the problem where the camera's imaging lens is modeled as "thin" and distortion free. The edge of the shell, as seen in the image, occurs when the principal ray of the imaging lens is tangent to the surface of the shell. By determining the height, h_i^*, of the imaged edge on the detector, the physical radius of the shell may be calculated by the following equation

$$R = \frac{\left|h_i^*\right| L}{\sqrt{\bar{d}_i^2 + \left(h_i^*\right)^2}}. \tag{7}$$

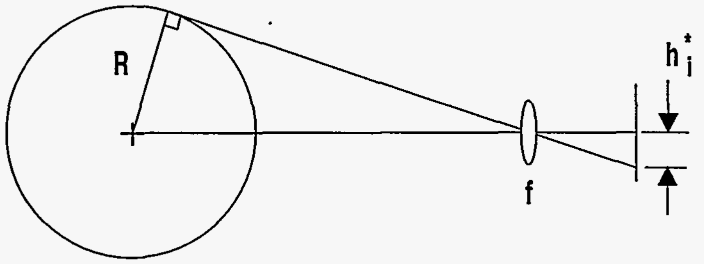

Figure 4. Edge ray condition used to determine the radius of the shell.

The physical height on the sensor is related to the pixel height by

$$h_i = n\,\Delta_i, \tag{8}$$

where n is the number of pixels from the center of the image to a point in the digital image, and Δ_i is the physical spacing of the detector elements.

The procedure for unwarping and tiling the views from multiple cameras can be summarized as:

1) Determine the physical height of the shell edge image on the detector array. An image processing technique is used to locate the edge in the digital image. Equation (8) is used to compute the physical height of the edge on the sensor array.

2) Compute the physical radius R of the shell using Eq.(7).

3) Determine the number of pixels N_{max} in the final corrected image to the cross-over point between adjacent images using Eq.(6).

4) For the arc-lengths in the final image given in Eq.(5), determine the corresponding pixel location in the original image and estimate the image gray level.

The lens has been modeled as an ideal "thin" lens with no distortion. Low distortion lenses can be purchased. It is possible, however, to include the effects of lens distortion in the model as presented above. Solving for the physical radius of the shell, however, is more difficult.

This process is depicted in Fig. 5 with three images from each individual camera acquisition and a final resulting circumference image.

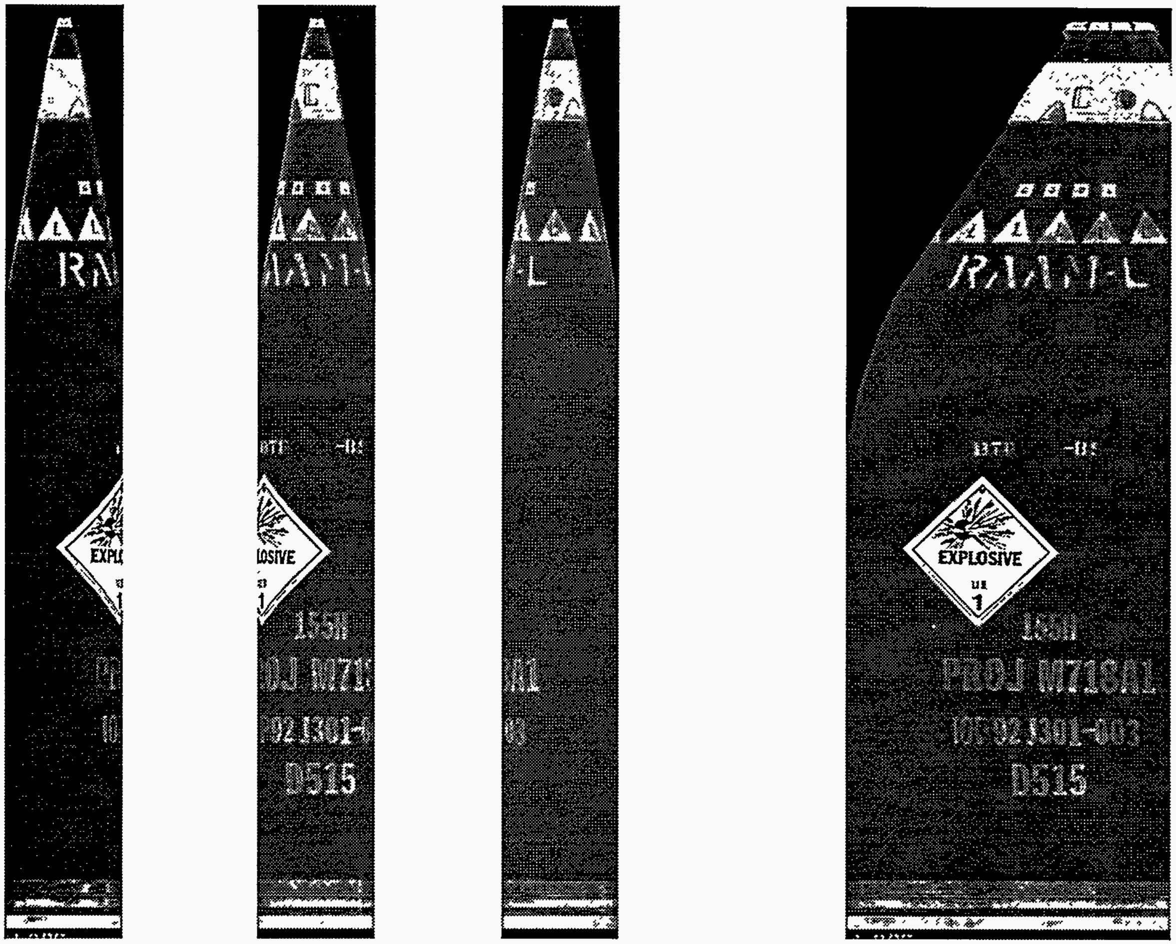

Figure 5. Three individual images warped and the corresponding composite.

4. EXPERIMENTAL SETUP

An experimental test stand was constructed and the optical and image processing hardware configured to enable testing and verification of the proposed algorithms. The images were acquired using a Dalsa 2k line scan camera and a Datacube MV-200 VME image processing board with a digital input module. A linear slide was used to translate the camera over the full length of the ammunition. The drive motor for the linear slide was connected to an optical encoder which generated pulses for the image row counter on the digital input module. Figure 6a shows the general configuration of the ammunition, camera and lights. An additional motor was used to rotate the ammunition through 360° in four discrete steps to obtain the individual images required for the warp and tile operation.

The ammunition shell must be illuminated in order for the camera system to image the shell surface. It is important to deliver sufficient light energy to the surface so that the detectors will have adequate light levels. The apertures on the lenses may be opened larger to increase the signal level but only to the point where the depth of field is still acceptable. The lighting system used with the system prototype consists of two circular fluorescent lamps placed above and below the camera's line of focus on the shell. Figure 6b illustrates the geometry of the lighting system. The two lamps, above and below the line of focus, are used to eliminate shadowing effects. The circular geometry of the lamps matches the cylindrical shape of the ammunition shell. It provides uniform lighting around the shell because of the symmetry. In addition, since the light source directly illuminates the shell there are no losses from intervening optical elements such as an optical fiber bundle.

The light irradiance at the sensor can be increased if the fluorescent bulbs are moved closer to the line of focus, however, the bulbs must far enough apart to avoid specular reflection into the camera. Specular reflection into the camera is most likely to occur on the taper of the shell as Fig. 6b illustrates.

The MV-200 board was used in combination with a Motorola MVME 167 single board computer and LynxOS real time operation system to perform all control and processing operations. Figure 7 shows the major hardware components of the test stand.

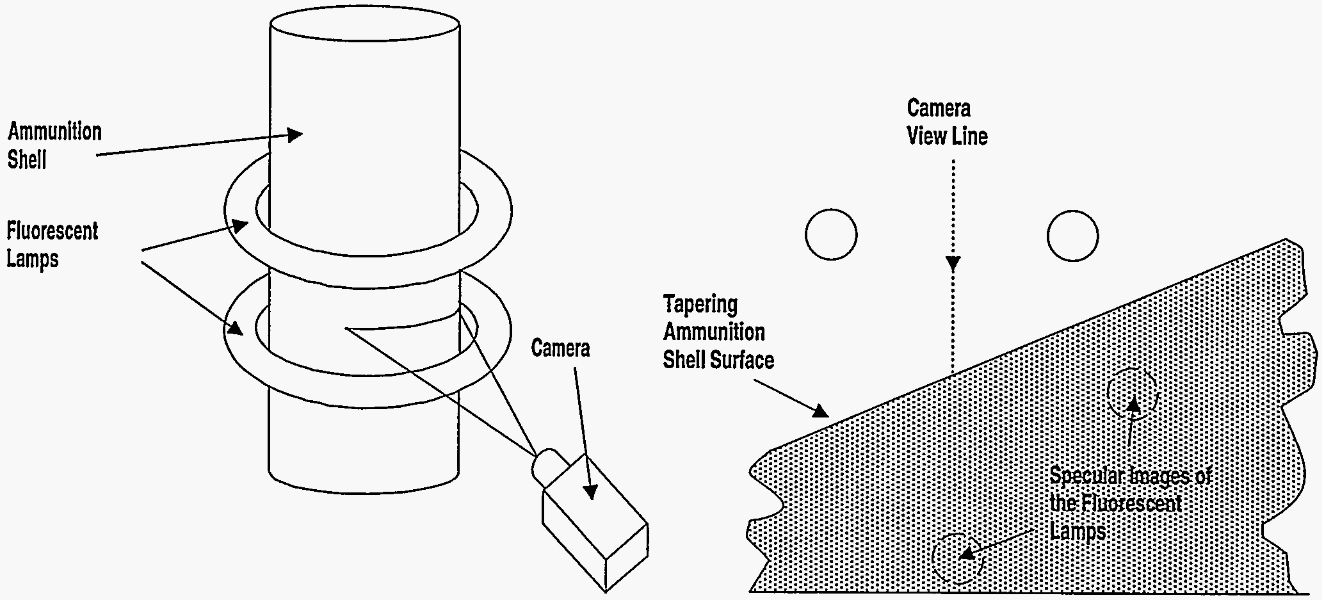

a. **b.**

Figure 6. a. Schematic of the main components of the image acquisition system. b. Specular reflection into camera due to narrow spacing of the fluorescent lamps.

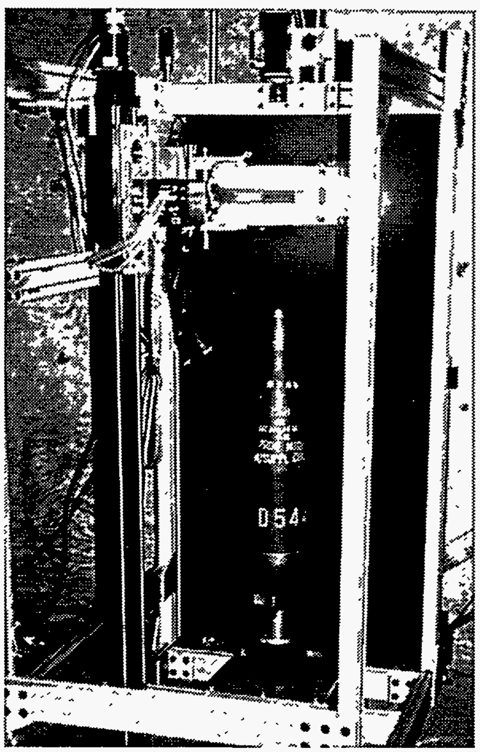

Figure 7. Photograph of the test stand during a trial of the system at the Army's Yuma proving grounds.

5. RESULTS

The results of applying the algorithms described in section 4 for the warping and tiling of the four individual camera images were very successful. This was evident by analyzing the resulting images using the classification and OCR algorithms. The image shown in Fig. 8 is representative of the entire set of ammunition rounds acquired during a trial at the Army's Yuma proving grounds. A total of 48 unique circumference images have been generated for further analysis.

The process of generating the parameters for the analytical expressions given in Eqs. 1, 6, and 7 proved to be somewhat time consuming. The main problem is determining the true focal length and magnification of the optical system. These parameters were determined via a calibration procedure and the specified nominal projectile radius (body section) given in drawings. A parameter that required experimental determination was the distance to the object plane. The calibration procedure used for the alignment of the camera did not include a section to measure this distance explicitly, so it was estimated.

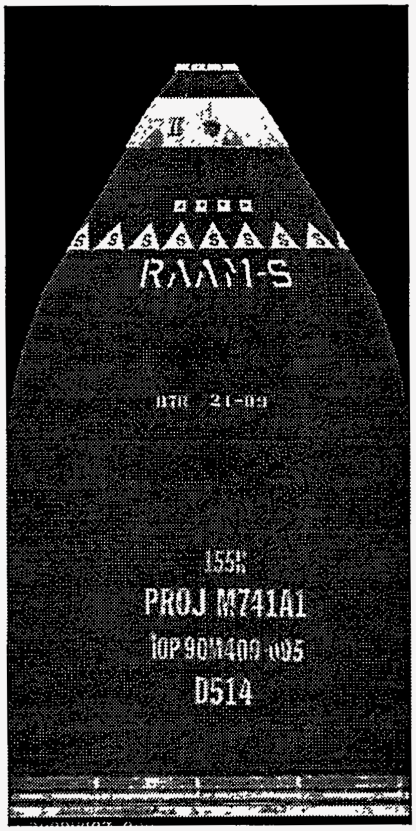

Figure 8. Example complete circumference image of a typical ammunition round acquired during testing.

6. CONCEPTUAL DESIGN

A conceptual design for a fieldable unit was generated using the information gained during the trials and requirements for the ammunition identification system. The production system uses a set of line-scan cameras, located around a portion of the vehicle's upload conveyor, to image the projectile as it moves across a gap approximately 15 cm wide. Four cameras are situated in a tight ring around the conveyor and the image path is folded to project onto the projectile's surface. Figure 9 shows a drawing of this design.

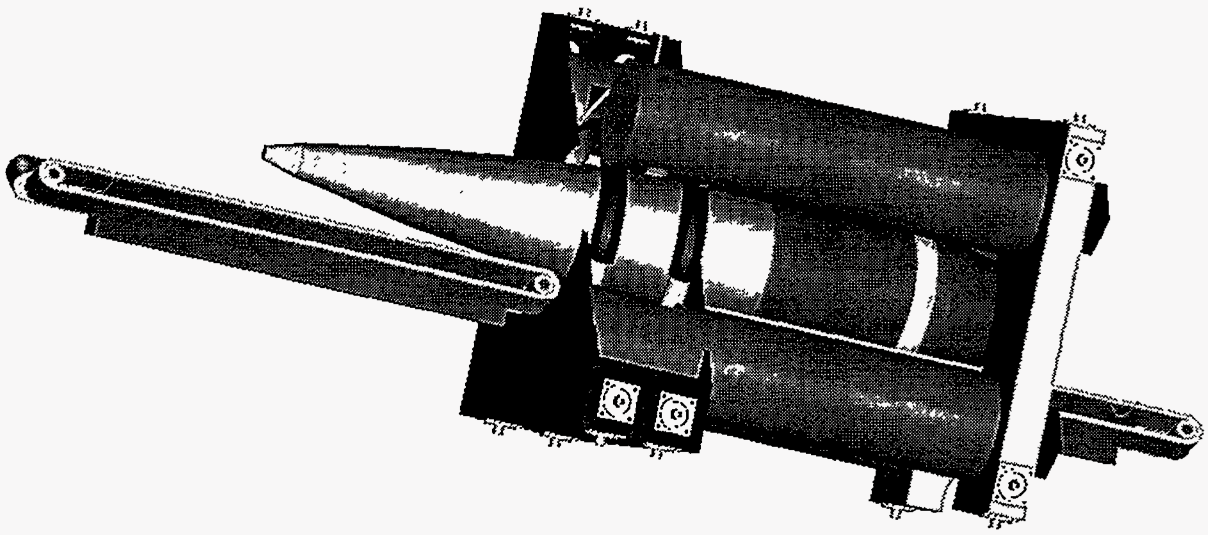

Figure 9. Mechanical design of a production identification module showing four imaging tubes and the conveyor belts used to move the ammunition.

7. CONCLUSIONS

The concept put forth in this report meet many of the functional, performance, and form-factor requirements of the Crusader ammunition identification system. Concepts for full ammunition identification have been developed and tested using actual data gathered using a development test stand. Some challenges for this type of system have also been identified and potential solutions presented.

The axial scan method using several cameras was proven to be a realizable approach to generation of the circumference image. The conic section of the projectiles proved to be a challenge to correct for the distortion and tile together at the appropriate locations. It was discovered that an accurate radius measurement along the length of the projectile was necessary for the warping/tiling operation. It was shown that the radius measurement could be made from the actual acquired raw images themselves.

ACKNOWLEDGEMENTS

The authors would like to thank the staff of the Army's Program Manager - Crusader for their support of the development effort and members of the United Defense team who provided input during the conceptual design phase.

REFERENCES

1. P. van Wie and M. Stein, "A Landsat digital image rectification system," *IEEE Trans. Geosci. Electron.*, **GE-15**, pp. 130-147, 1977.
2. D. Steiner and M. E. Kirby, "Geometrical referencing of Landsat images by affine transformation and overlaying of map data," *Photogrammetria*, **33**, pp. 41-75, 1977.
3. J. R. Muller, P. Anandan, and J. R. Bergen, "Adaptive-complexity registration of images," *Proc. IEEE Computer Society Conference on Computer Vision and Pattern Recognition*, pp. 953-957, IEEE, Los Alamitos, 1994.
4. J. A. Bieszk and I. Fram, "Automatic elastic image registration," *Proc. Computers in Cardiology*, pp. 3-5, IEEE, Los Alamitos, 1987.

5. L. M. Buur, D. L. Wilson, and D. D. Faul, "Registration of digital subtraction peripheral angiography images," *Proc. Northeast Bioengineering Conf.*, pp. 69-70, IEEE, Piscataway, 1990.

6. C. Frederick and E. L. Schwartz, "Conformal image warping," *IEEE Comput. Graphics Appl.*, **10**(2), pp. 54-61, 1990.

7. Y. Nakazawa, T. Komatsu, and T. Saito, "High-resolution image acquisition based on temporal integration with hierarchical estimation of image warping," *Proc. IEEE Int. Conf. on Image Proc.*, **3**, pp. 244-247, 1995.

8. J. W. Monaco and J. T. Mark, "Image warping approach to image sequence interpolation," *Proc. IEEE Int. Conf. on Image Proc.*, **1**, pp. 338-342, 1994.

9. R. C. Gonzalez and R. E. Woods, *Digital Image Processing*, pp. 296-302, Addison-Wesley, Reading, 1992.

10. G. Wolberg, *Digital Image Warping*, IEEE Computer Society Press, Los Alamitos, 1990.

11. K. W. Tobin, M. A. Hunt, W. B. Jatko, "High resolution three-dimensional image registration," *Proc. SPIE Applications of Digital Image Processing XII*, **1153**, pp. 541-551, 1989.

12. N. Arad and D. Reisfeld, "Image warping using few anchor points and radial functions," *Computer Graphics Forum*, **14**(1), pp. 35-46, 1995

13. G. F. McLean, "Image Warping for calibration and removal of lens distortion," *Proc. IEEE Pacific Rim Conf. on Comm., Comp. and Signal Proc.*, pp. 170-173, IEEE, Piscataway, 1993.

14. D. F. McAllister, "Digital correction of keystoning caused by image translation," *Proc. SPIE Stereoscopic Displays and Virtual Reality Sys.*, **2177**, pp. 97-107, SPIE, Bellingham, 1994.